Effects of Forward Blade Sweep on the Three-Dimensional Flow in Axial Flow Rotors

CEST02_215

ABSTRACT

Computational study was carried out in order to review the outcome performance of forward sweep (**FSW**) and unswept (**USW**) in axial flow rotors for incompressible flow.

The effects of sweep applied to rotor of axial flow turbomachines were investigated by means of applying computational fluid dynamics (CFD) tools. Low-aspect-ratio rotors of forward has been studied and compared to unswept datum rotors, at one flow rate and different spanwise locations. The studies have been carried out on both rotors, by means of developing structured fully hexahedral meshing of the entire computational domain. The structured meshing technique offers the moderation of cell number and skewness, and makes possible cost-effective CFD investigations. Investigation of inlet flow field was carried out at the design flow rate.
It is concluded that at the design point forward-swept rotor increases the total pressure rise for the most part of the blade span, especially at the blade hub as well as the efficiency is improved near the tip and near the hub compared to unswept rotor.

Keywords: Axial flow turbomachinery, Blade sweep, Three-dimensional turbomachinery flow, CFD, Structure meshing, Local efficiency.

1. Introduction

Developed geometry of blades by means of sweep, dihedral, skew or twists along the blade span are nowadays more significance. Blade design is receiving more attention by the designers as a viable means to reduce losses and improve efficiency. The recent designs of swept blades in axial fan rotors provide a significant improve in fan performance. Early researches on these blades were primarily focused on aerodynamic performance characterization of blades. Hurault et al. [1] used both CFD coupled with semi-empirical models to investigate the pressure fluctuations in axial flow fans. In this study, a computer program is used to study and examine the effects fan blade geometry on the Three-Dimensional (3-D) flow in the use of blading methods, such as sweep (airfoil movement parallel to the chord line). A comparative study by means of a computational Fluid Dynamics (CFD) tool for Forward Sweep (**FSW**) and Unswept (**USW**) blades is carried out. Figure1 shows the front outlook of these blades.

USW blade FSW blade

Figure 1. Front view of USW and FSW blades

Only at the design flow rate, low-aspect-ratio rotor of FSW sweep has been studied and compared to unswept datum rotor, and different spanwise locations. Bizjan et al. [2] studied the effect of blade tip geometry on axial fan operation in four different operating points along with the underlying flow energy conversion and dissipation mechanisms. However the most key effect of sweep is in the reduction of endwall losses. Experiments and numerical results have shown a positive sweep at the hub to reduce secondary flow losses. [3]

Forward sweep presents a potential for the improvement of aerodynamic performance and total efficiency [4 , 5]. Jin et al. [6] experimentally and numerically investigated the performance of a small axial fan with novel circumferentially skewed blades. They found that the forward-skewed blades were able to control the tip leakage flow and low energy flow.

Numerical simulation was carried out using ANSYS Student Release 17.2, with finite volume method. The goal of this study is to achieve additional knowledge about the effects of the forward sweep that not provided by the existing literature and filling this gap.

2. Computational methodology

2.1. Cascades model

Nowadays, the blade design can be organized in such a way that the blades are assembled and arranged either in linear or annular cascades; although more difficulties in the case of annular cascades design and meshing are found with this kind of cascades. Annular 3D cascades were selected for the computational models in this study. With the aim of concentrate only on the effect caused by the forward sweep, the blade profile is identical at every spanwise section in each cascade as illustrated in Figure 2.

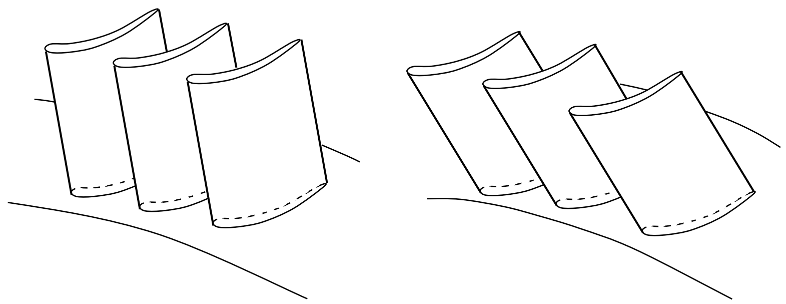

a) 3D annular cascade b) 3D annular cascade with sweep

Figure 2. Type of cascades

Utilising the features of the annular cascade configuration, boundary conditions of periodicity were applied, as presented in Figure 3.

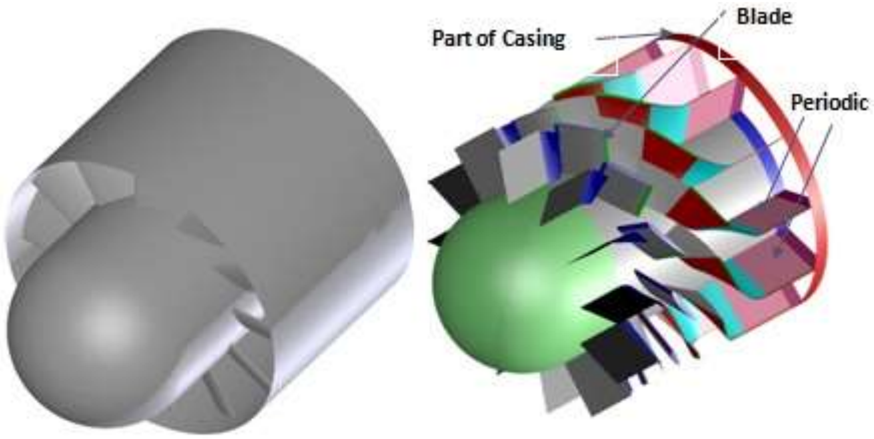

a) without periodic walls b) showing virtual periodic walls

Figure 3 View of annular cascades.

2.2. Sweep configurations

Different definitions of sweep have been adopted in the literature. The used definition in this paper is that, the Sweep is a non-radial blade stacking technique. Sweep is forward or backward if a blade section at a given radius is upstream or downstream of the adjacent blade section at lower radius respectively [7], i.e. It is provided if the blade sections of a datum blade of radial stacking line (RS) are displaced parallel to the chord. Our case study acquired as forward sweep when a higher span section was moved in the upstream direction relative to the lower section.

The stacking line (SL) is a connecting line through center of gravity for every blade airfoil sections from hub to tip. The chord line is the straight line connecting the two points of leading edge (LE) and trailing edge (TE) of each blade section as sketched in Figure 4

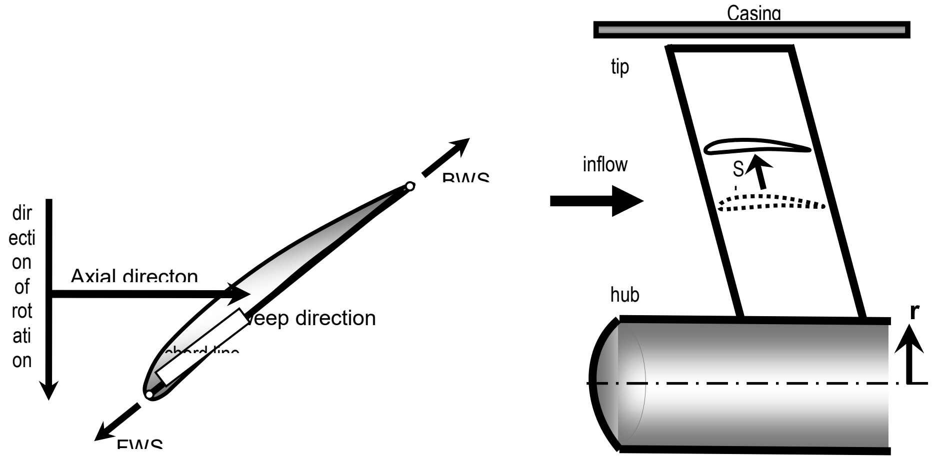

a) Direction of sweep b) Schematic drawing for FSW

Figure 4. Sweep direction and schematic drawing for FSW

The sweep angle was defined as the angle between the leading edge of the cascade and the radial direction in the chordwise direction. FWS blade sections of C4 (10%) profile along the entire span were built with spanwise constant sweep angle with 3.5 degree on the basis of the data of Vad, et al. [8]. The Reynolds number used is approx. 1.074×10^6.

3 CFD technique

3.1geometry construction

Commercial available finite-volume ANSYS-17.2 code is used. The study geometry in this work has 12 blades in casing of diameter 2000 *mm*, the tip clearance (ν) is 5% span with Hub-to-tip ratio (τ) of 0.6. At the beginning, 3-D volumetric domain around the one blade of axial flow fan was constructed. The domain divided into three parts. The first part starts from the inlet of the fan until the end of the half sphere shaped inlet corn. The second one starts from the end of the first one until the front of the hub and the last one contains the hub and the blade part. Typical computational domain for USW rotor is presented in Figure 5.

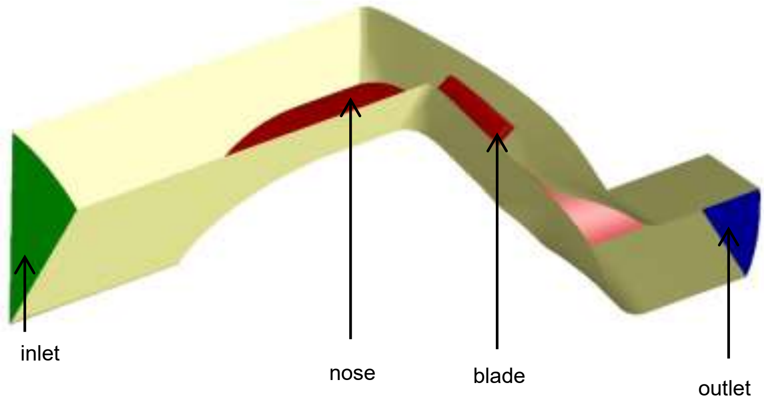

Figure. 5. Computational domain for USK rotor
(The casing is hidden for clarity)

3.2 Meshing

Multiblocks structured grids technique is provided by means of splitting the domain into several volumes. These volumes were meshed separately. Using adequate hexahedral meshes for the whole geometry of both rotors are achieved. 2-D structured meshes take place in two essential forms H-grids and C-grids as the automated mesh deformation scheme is presented Ref. [9]. Instead of meshing the whole rotor geometry, periodicity has been taken into consideration, this is to avoid the mesh size and time consuming. Figure 6 shows a smooth hexahedral structural grid at the LE and TE of the blade as a part of multi-blocks.

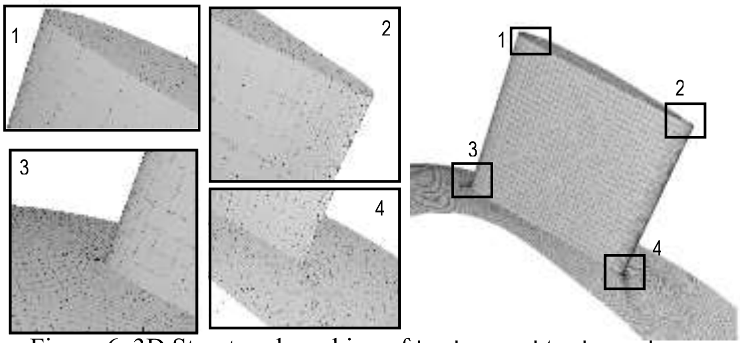

Figure 6. 3D Structured meshing of leading and trailing edges.

About 50 % of the total cells are located at the refined domain in the vicinity of the blade. The domain consists of 31 blocks. The total number of cells in the structured grid is approx. 270,000 hexahedral cells for both rotors. Figure 7 shows representative details of the meshing for USW rotor.

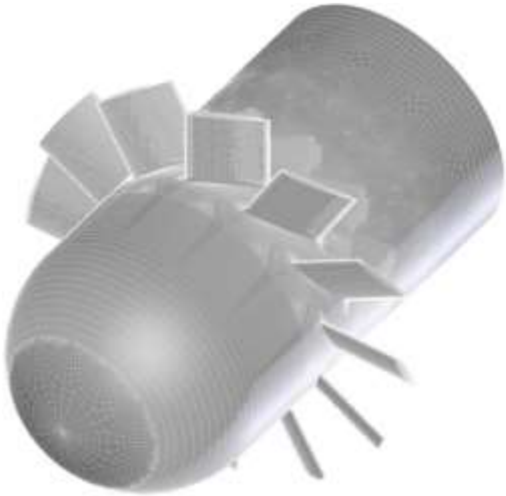
Figure 7. Meshing details for USW rotor

The boundary Conditions are used as follows, the inlet is set as a velocity of 9.2 [m/s], outflow as Outlet, the turbulence model set as standard k-ε model with enhanced wall treatment. The y+ values mostly fell within the range of 30 to 100. Typical computations required approximately 5000 iterations. The solutions were considered converged when the scaled residuals reached to 10^{-8}.

4 Results and Discussion

The inlet and outlet planes have positioned closely to the blade at the axial direction shown in Figure 8a, another investigation located at 20% and 90% of the spanwise measured from the hub are shown in Figure 8b.

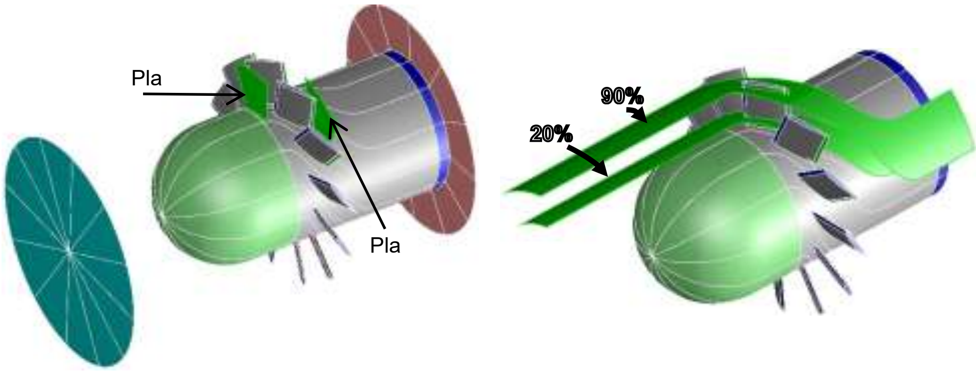

a) input and output planes b) 20% and 90 % span

Figure 8. Location of results

The reference velocity (u_{ref}) or (u_t) in [m/s] can be defined as blade tip speed = (d_t π n) where, d_t is the blade tip diameter and n is the rotor speed (in revolutions per second), fraction of span(σ) is the radial distance from the hub divided by blade span height, thus the definition of local flow coefficient (φ) is the ratio of axial velocity (v_x) to u_t.The inlet axial velocity for FSW is increased at the midspan especially at SS and is reduced at lower radii as shown Figure 9a, this was detected for FSW rotors by Meixner [10]. As shown Figure 9b the consequences of this is FSW near-tip blade extends into the upstream relative flow field, and holds a work in advance compared to the lower radii of blade sections.

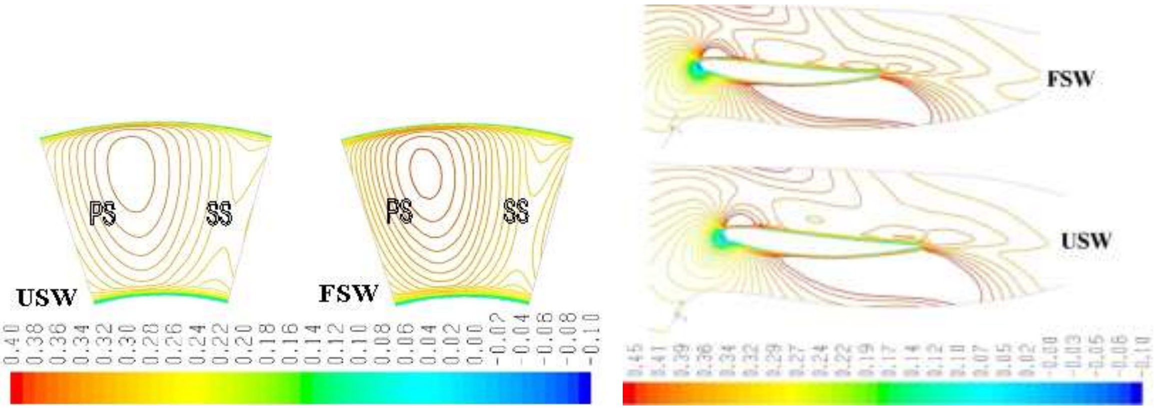

a- at inlet plane b- at 90% span

Figure 9. Distribution of local axial velocity

Figure 10 shows the distribution of static pressure coefficient Cp on the SS, forward sweep moderates radial outward flow at the SS surface. The isobars are slightly inclined ahead toward the LE and accumulated closing the blade tip for FSW than for USW rotor. The same manner can be attached with the consequence of the total pressure rise as shown in Figure 13b, similar effects of radial flow have been explained in [5].

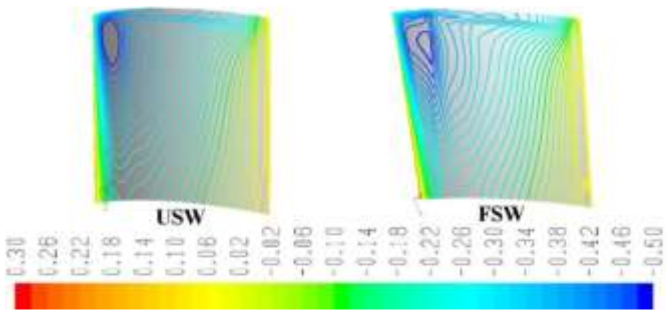

Figure 10. Distribution of static pressure coefficient Cp on the SS

The definition of local radial flow coefficient (φ_r) is the ratio of axial velocity (v_r) to u_t. In view of the fact that, the endwall boundary viscosity can affect the flow through the blade span. Due to blockage, the radial flow occurs along the span. Figure 11 shows that forward sweep decreases radial velocity near the blade tip and it on the range of lower 70% spanwise, whereas unsweep blade has just the contrary of that.

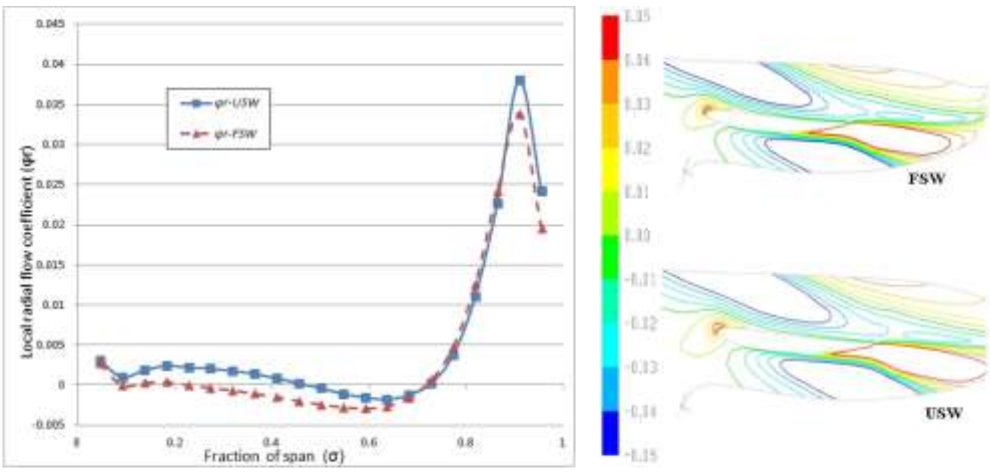

a- Outlet pitchwise averaged data

b- at 90% span

Figure 11. Distributions of local radial velocity.

The definition of ideal total pressure rise coefficient (ψ_{id}) is $\psi_{id}=\Delta p_{t\,id} / (\rho\, u_{ref}^{\ 2}/2)$. Where, $\Delta p_{t\,id} = \rho\, r\, \omega\, v_{u2}$, v_{u2} is the tangential pitchwise mass-averaged tangential velocity, r is radial coordinate, ω is rotor angular speed and ρ is the air density.

For both rotors, spanwise increase of an ideal total pressure rise dominates along the span, according to the concept of “controlled vortex” design (CVD), the rotors are of “controlled vortex” design, resulting increasing Euler work and blade circulation along the dominant part of span in a prescribed manner [3]. Figure 12a presents the distributions of ideal total pressure rise at the design flow rate. This figure shows forward sweep increases ideal total pressure rise at the dominant part of the blade span, whereas at 90% of the spanwise unswept blade has the same effect. Wadia et al.[11] pointed out that the main advantages of forward sweep is decreased loading at the fan tip. As the ideal total pressure rise an axial velocity, FSW performs increased Euler work compared to USW above midspan. However FSW decreased Euler work compared to

USW below midspan as showing in Figure 12b. The Euler work having these changing is due to non-radial blade stacking, as was detected also by Clemen et al. [12].

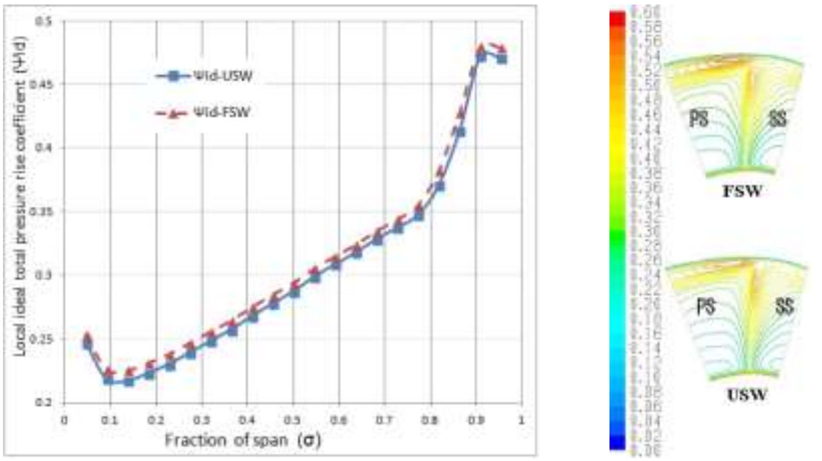

a- Pitchwise averaged data b- at outlet plane

Figure 12. Distributions of local ideal total pressure rise at the design flow rate

The definition of the local total pressure rise coefficient (ψ) is Δp_t / (ρ u_{ref} ^{2}/2), where Δp_t is the pitchwise mass-averaged local total pressure rise. Figure 13 shows that, most of blade span response to increases the total pressure rise with increasing sweep except the range of 85%-90% spanwise. The aerodynamic advantages of forward sweep can be utilized while improving the mechanical properties of the blade. The total pressure rise of forward sweep is observed for FSW along a large part of the spanwise range, as agreed in Cros et. al.[13].

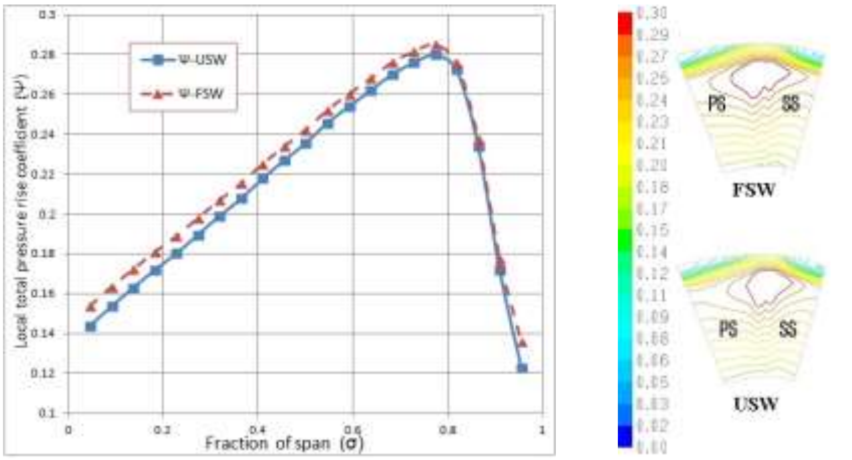

a- Pitchwise averaged data b- at outlet plane

Figure 13. Distributions of local total pressure rise at the design flow rate.

The total pressure loss coefficient (ω) can be defined $\omega = \psi_{id} - \psi$. No different effects of forward sweep compared to unswept on the total pressure loss. This is due to the balancing of an ideal pressure rise with the total pressure rise; beyond this angle of sweep, forward sweep may be has a different effects on the fan performance. Utilizing the local total pressure loss is increased at the blade tip by applying the forward sweep, this increasing causes to decrease of local total efficiency at the endwalls. As observed in Figure 14. The pressure loss is highly increased in the region more than 80% span for both rotors; this is due to exist of the tip clearance.

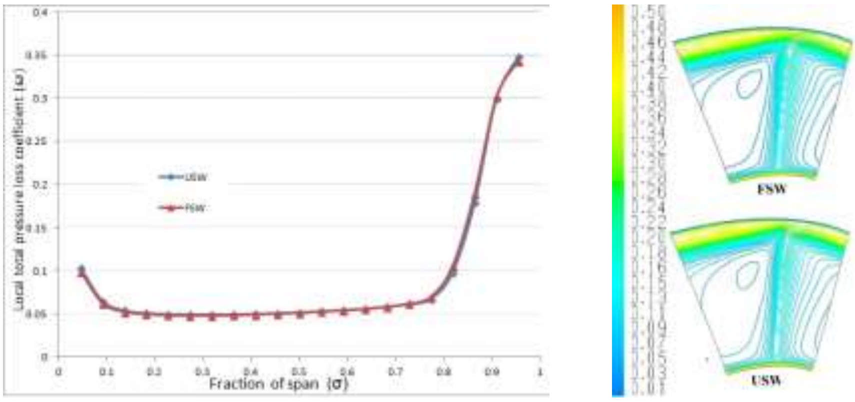

a- Outlet pitchwise averaged data b- at outlet plane

Figure 14. Distributions of local total pressure loss coefficient

The local total efficiency (η) can be defined as $\eta = \psi / \psi_{id}$. The effect of forward sweep on efficiency is negligible within the range of 40% - 90% spanwise of the blade; beyond this range, forward sweep has a beneficial effect on increasing the efficiency. Effect of sweep on the efficiency response is more predominant near the hub and tip as seen in Figure 15. As mentioned by Passrucker et. al.[14] that the calculation as well as the measurement show an increased efficiency for the forward swept rotor compared to a radially stacked rotor.

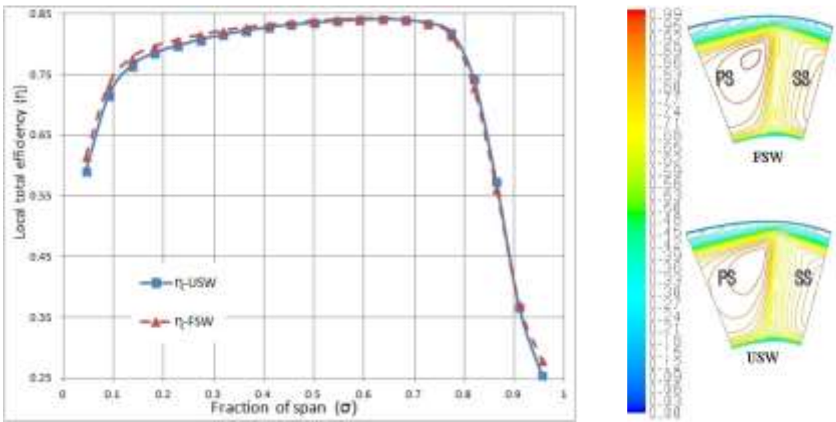

a- Outlet pitchwise averaged data b- at outlet plane

Figure 15. Distributions of local total efficiency at the design flow rate

5 Conclusions

The purpose of this study is to examine the effects of forward sweep applied to rotor of axial flow turbomachines at the design point by using CFD tools. In this paper, it is concluded that, forward sweep rotor exhibits improve on the local total efficiency near the hub and the blade tip at the design rate. These results, therefore, demonstrate that the FSW rotor gives a potential to increase the total pressure rise in the dominant of spanwise except the range of 85%-90% span.

It is pointed out that generally forward sweep has no different effects on the total pressure loss compared to unswept rotor. Since, the total pressure loss profile has been found practically identical for both rotors and there is no different effect on the total pressure loss by using one angle of forward sweep. It is recommended that, additional alternative angles of sweep on forward sweep should be investigated for further results.

References

[1] Hurault, J., Kouidri, S., & Bakir, F. (2012). Experimental investigations on the wall pressure measurement on the blade of axial flow fans. *Experimental Thermal and Fluid Science*,40, 29-37.

[2] Bizjan, B., Milavec, M., Širok, B., Trenc, F., & Hočevar, M. (2016). Energy dissipation in the blade tip region of an axial fan. *Journal of Sound and Vibration*, 382, 63-72.

[3] S. J. Gallimore, J. J. Bolger, N. A. Cumpsty, M. J. Taylor, P. I. Wright, and J. M. M. Place. The Use of Sweep and Dihedral in Multistage Axial Flow Compressor Blading-Part II: Low and High-Speed Designs and Test Verification. *Journal of Turbomachinery*, 124(4): 533-541, 2002.

[4] Vad, J., Kwedikha, A. R. A., Horváth, Cs., Balczó, M., Lohász, M. M., and Régert, T., "Combined Aerodynamic Effects of Controlled Vortex Design and Forward Blade Skew in Axial Flow Rotors". Proceedings of the Institution of Mechanical Engineers – Part A: *Journal of Power and Energy*, 2007, Vol. 221, pp. 1011-1023

[5] Yamaguchi, N., Tominaga, T., Hattori, S., and Mitsuhashi, T., 1991, "Secondary-Loss Reduction by Forward-Skewing of Axial Compressor Rotor Blading," presented at *Yokohama International Gas Turbine Conference*. Yokohama, Japan, pp. II.61 - II.68

[6] Jin, G.; Ouyang, H.; Du, Z. Experimental investigation of unsteady flow in axial skewed fans according to flow rates. *Exp. Therm. Fluid Sci*. 2013, 48, 81–96.

[7] Van Den Braembussche, R. A. and Vad, J. "Challenges in optimisation of axial flow turbomachinery blades for 3D flow, including sweep and dihedral effects. In Modelling Fluid Flow", Springer Verlag Heidelberg, 2004, pp. 99-103.

[8] Vad, J., Kwedikha, A. R. A., Kristóf, G., Lohász, M. M., Rábai, G., Rácz, N. and Watanabe, K. , 2005, "Effects of blade skew in an axial flow rotor of controlled vortex design." 6th *European Conference on Turbomachinery* Fluid Dynamics and Thermodynamics, Lille Proceedings pp. 46-55.

[9] Muir, E. R. and Friedmann, P. P., "Unsteady Aerodynamic Analysis of a Bird-Damaged Turbofan,"AIAA Paper No.2013-1773, Proceedings of the 54th AIAA/ASME/ASCE/AHS/ASC Structures, *Structural Dynamics, and Materials Conference*, Boston, MA, April 2013

[10] Meixner, H. U. Vergleichende LDA-Messungen an ungesichelten und gesichelten Axialventilatoren. Dissertation Universität Karlsruhe, VDI-Verlag, Reihe 7: Strömungstechnik, No. 266, Düsseldorf, 1995.

[11] Wadia AR, Szucs PN, Crall DW. Inner workings of aerodynamic sweep. *J Turbomach* 1998;120(4):671–82.

[12] Clemen, C., Gümmer, V., Goller, M., Rohkamm, H., Stark, U. and Saathoff, H., 2004. "Tip-aerodynamics of forward-swept rotor blades in a highly-loaded single-stage axial-flow low-speed compressor." *10th International Symposium on Transport Phenomena and Dynamics of Rotating Machinery* (ISROMAC10), Honolulu, Paper No. 027. (CD-ROM Proceedings)

[13] Cros, S. and Carbonneau, X., 2009, "Computational Study of the Aerodynamic. Impact of Stall Margin Improvements in a High. Tip Speed Fan", Proc. 8th *European Turbomachinery Conference*, Graz, Austria, pp. 401-409.

[14] Passrucker, H., Engber, M., Kablitz, S., Hennecke, D.K.: The Effect of Forward Sweep in a Transonic Compressor Rotor. In: Proceedings of the 5th *European Conference on Turbomachinery*, Fluid Dynamics and Thermodynamics, pp. 141–150 (2003)